

NASA Grant NGR-36-003-054

FUNDAMENTAL STUDIES FOR THE DEVELOP-  
MENT OF POLYETHYLENE TEREPHTHALATE  
AS A CRYOGENIC LINER MATERIAL

Semi-annual Report  
October, 1966

N67-16088

Part I

MECHANICAL RELAXATION BEHAVIOR

OF PET FROM 4.2 TO 280°K

by

I. Kuriyama and Eric Baer

## INTRODUCTION

Several papers have been published concerning the effect of temperature (ranging from 77°K to the melting point) and frequency on molecular motion in PET. Farrow, Ward and coworkers<sup>(1-3)</sup> investigated the transitions in a series of polymethylene terephthalate polymers using dynamic mechanical, nuclear magnetic resonance, infrared and x-ray techniques. In each of these polymers a first order melting transition was observed and two second order transitions labelled  $\alpha$  and  $\beta$  in descending order of temperature; where normally  $\alpha$  corresponds to the glass transition temperatures. The NMR results indicated that the  $\beta$  transition is restricted to very small intramolecular motions, whereas the  $\alpha$  transition is associated with large segmental movement in the amorphous regions. Illers and Brewer<sup>(4)</sup> also have investigated the shear,  $G'$ , and the loss,  $G''$ , moduli in polyethylene terephthalate, PET, in the low frequency range between 90°K and melting. They similarly reported two major relaxation maxima; a sharp almost symmetrical peak at approximately 353°K ( $\alpha$  peak,  $T_g$ ) and an asymmetric peak near 208°K. The complex  $\beta$  peak was shown to be almost insensitive to crystallinity and it was suggested that this maxima is partially due to the onset of molecular motion of the  $\text{COO}$ -groups in both the trans and gauche positions. In addition, a definite shoulder attributed to the motion of  $\text{CH}_2$  groups was observed around 108°K. In order to trace the molecular origin of these maxima,

various investigators<sup>(4-6)</sup> have used plasticizers which can markedly affect the shape of the loss modulus -- temperature curve as well as the temperatures of the relaxation maxima.

The objectives of this investigation are to study the relaxation processes in PET and related polymers ranging from liquid helium to room temperature. Particular emphasis is being placed on relaxation processes occurring between 4 to 90°K since these molecular motions may be extremely important in understanding and improving the ductility of these materials at liquid hydrogen temperatures (20.6°K). Furthermore, previous relaxation studies, which were carried out starting at liquid nitrogen temperatures, did not consider the marked effect of orientation on molecular relaxations at cryogenic temperatures. In this report, new relaxation maxima occurring below 110°K are reported as well as some preliminary results describing relaxations in the oriented state.

## EXPERIMENTAL

The experimental apparatus used was a torsion pendulum previously described in these reports which allows the measurement of the shear modulus,  $G'$ , and loss modulus,  $G''$ , down to 4°K. All runs were conducted at a frequency of 1.32 cycles/sec.

### Calculation of Shear and Loss Moduli

The equations used to calculate these moduli are well known. The logarithmic decrement,  $\Delta$ , is defined by the equation

$$\Delta \equiv \frac{1}{n} \ln \frac{a_0}{a_n} \quad (1)$$

where  $a_0/a_n$  is the ratio of the amplitude of one cycle to that of the n-th oscillation. The shear modulus of the sample,  $G'$ , was calculated from the approximate equation (about 1% error)

$$G' \simeq 4\pi^2 \frac{LM}{NP^2} \quad (2)$$

where  $L$  is the sample length,  $N$  is a form factor depending on the sample cross section dimensions,  $M$  is the moment of inertia of the pendulum and  $P$  the period of the oscillations. From  $G'$  and  $\Delta$ , the loss modulus,  $G''$ , was obtained using the relation

$$G'' = \frac{\Delta G'}{\pi} \quad (3)$$

### Reproducibility of Data

The reproducibility of data has been checked on several occasions. In Figure 1, the logarithmic decrement,  $\Delta$ , has been plotted as a function of temperature for amorphous unoriented PET. Two separate specimens were used with similar processing history. Both the shape of the loss peaks and the temperatures of the various relaxation maxima

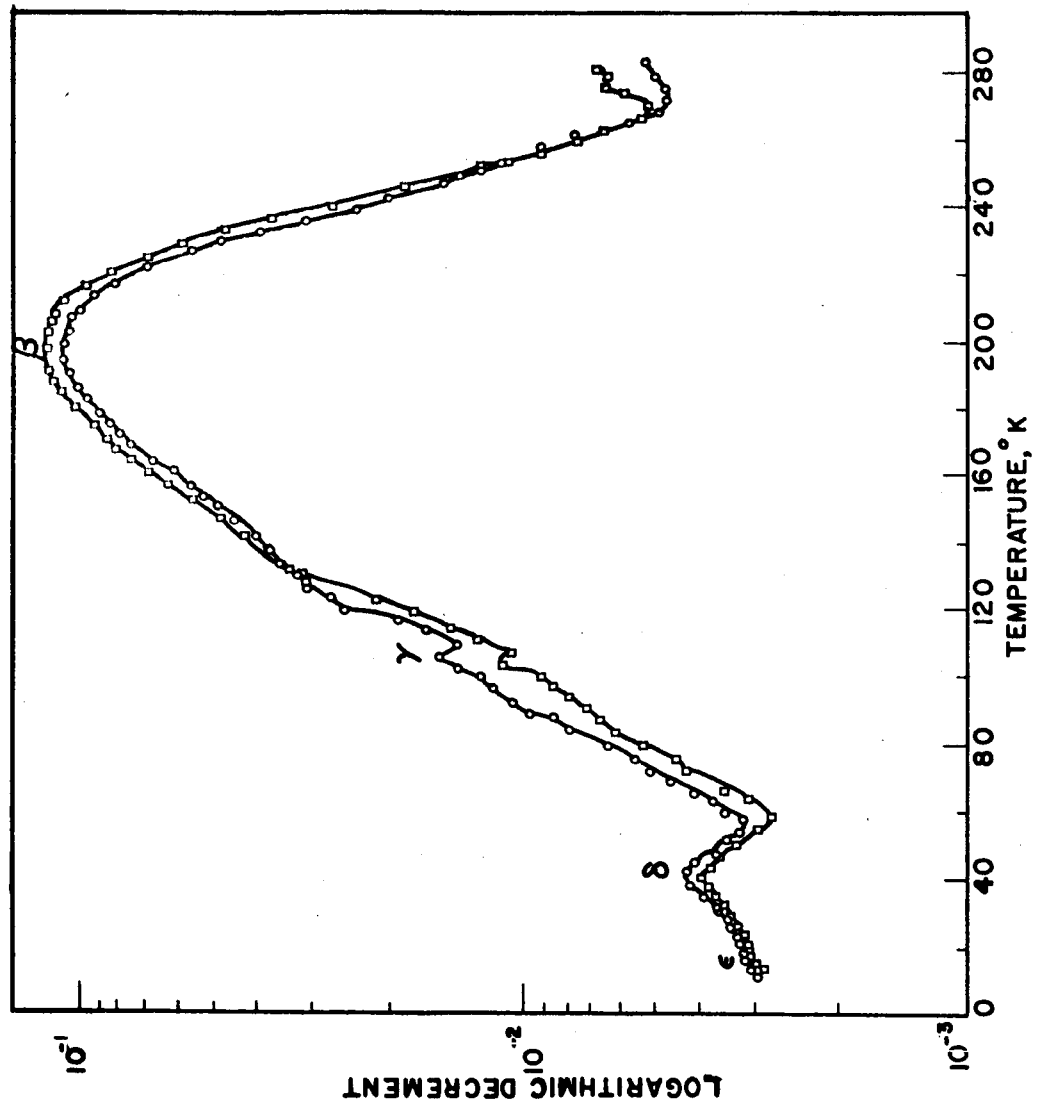


Figure 1.

are quite reproducible. However, the relative intensity varies somewhat between samples which is probably due to a combination of instrumental error and property variations between the test specimens.

#### Preparation and Crystallinity Measurements

Preparative conditions for PET samples used are summarized in Tables 1 and 2. The density was measured by the floatation method using carbon tetrachloride and M-heptane, and the per cent crystallinity calculated in the usual way using a unit cell crystal density of 1.455g/cc and an amorphous density of 1.331 g/cc.

Table 1  
Preparation and Calculated Crystallinities for  
Unoriented PET Film

Sample No.	Casting Method	Annealing Condition	Density g/cc	Crystallinity %
1	melted at 280°C for 3 min. and quenched into ice water	None	1.335 <sub>1</sub>	3.5
2	"	90°C, 25 hrs. in silicon oil	1.350 <sub>8</sub>	17.2
3	"	110°C, 10 hrs. in silicon oil	1.376 <sub>6</sub>	38.3
4	"	200°C, 30 min. in nitrogen	1.394 <sub>2</sub>	53.0
5	melted at 280°C for 3 min. and cooled- down slowly to room temperature	None	1.408 <sub>9</sub>	64.1

Table 2  
Preparation and Calculated Crystallinities  
for Oriented PET Film

Sample No.	Drawing Condition	Annealing Condition	Density g/cc	Crystallinity %
8	Uniaxial-drawn at 60°C (Draw ratio 6:0)	None	1.362 <sub>1</sub>	26.7
9	"	200°C, 30 min. in nitrogen	1.392 <sub>3</sub>	51.4
10	Simultaneous biaxial draw at 40°C (3:3)	240°C, 30 min. in nitrogen	1.401 <sub>1</sub>	58.6
11	Commercial Mylar; process history unknown	None	1.398 <sub>0</sub>	56.2
12	Biaxially oriented commercial Mylar C	None	1.391 <sub>7</sub>	51.2

## RESULTS AND DISCUSSION

Effects of Crystallinity on Mechanical Relaxation Spectra

The temperature dependence of the shear and loss moduli was studied with samples ranging in crystallinity from 3.5 to 64%. Typical results are shown in Figure 2 for two samples with substantially different crystallinities. A summary of the relaxation peaks observed with five specimens of unoriented PET at various levels of crystallinity is given in Table 3.

Three new relaxation maxima referred to as  $\gamma$ ,  $\delta$  and  $\epsilon$  have been observed at around 105, 41, and 20°K, respectively. Although the shape of the  $\gamma$  and  $\delta$  peak tend to sharpen appreciably with crystallinity, the peak maxima remain fairly constant. However, the initial results indicate that  $\epsilon$  peak is measurably effected by crystallinity. An additional relaxation peak designated as  $\epsilon'$  has been found near 9°K in the high crystallinity samples.

Work is currently underway to find the structural origins of these relaxation maxima. Wide and small angle x-ray, electron microscopy and I. R. measurements are underway to determine the overall morphology and the structural differences between samples. In addition, work will be started to determine whether cryogenic ductility can be related to these relaxation maxima.

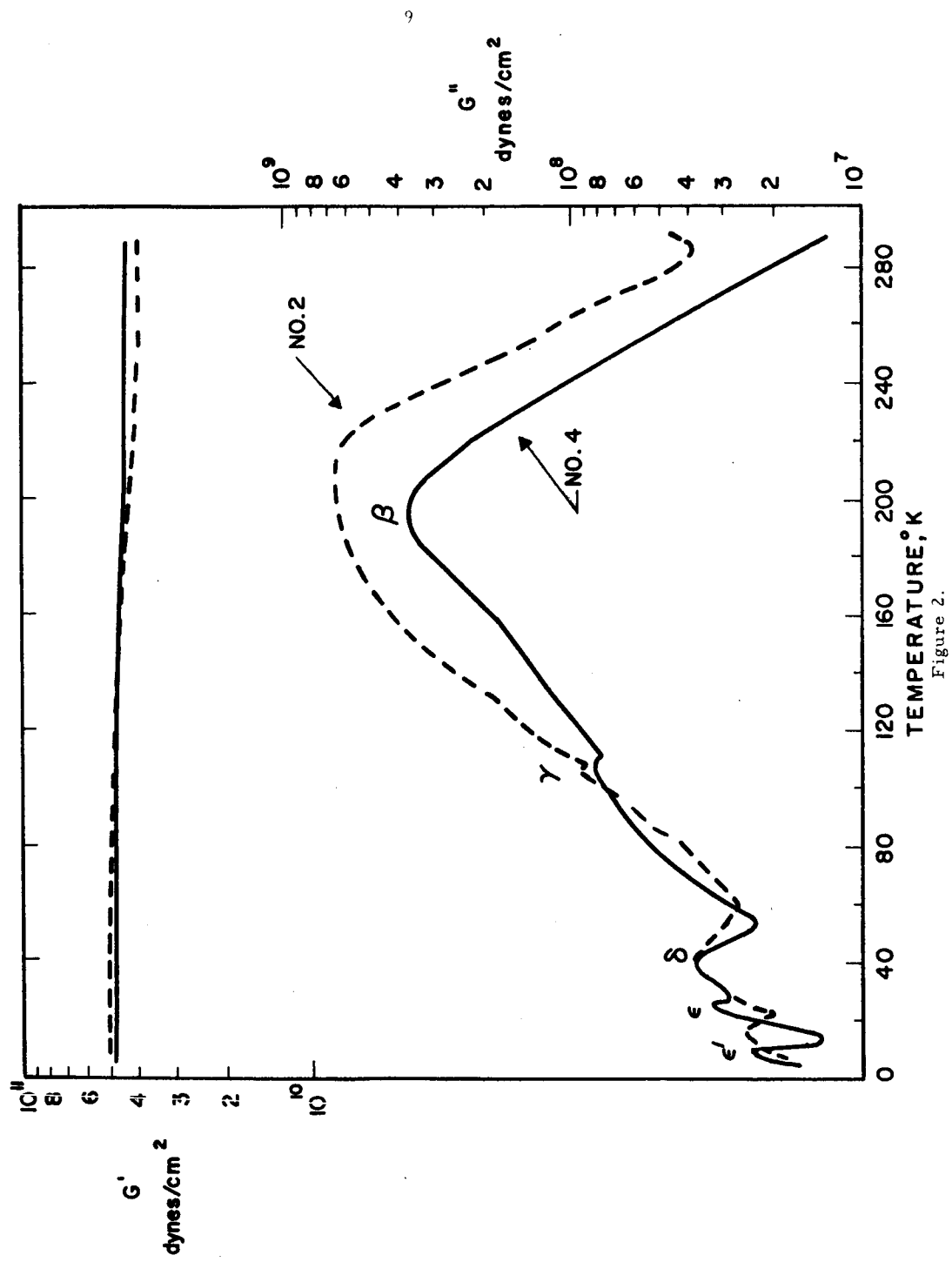


Figure 2.

Table 3  
Summary of Results Describing Relaxation  
Peaks Observed with Unoriented PET Film

Sample No.	$\beta$ peak			$\gamma$ peak			$\delta$ peak			$\epsilon$ peak		
	T °K	G' $\times 10^{10}$	G'' $\times 10^8$	T °K	G' $\times 10^{10}$	G'' $\times 10^7$	T °K	G' $\times 10^{10}$	G'' $\times 10^7$	T °K	G' $\times 10^{10}$	G'' $\times 10^7$
1	196	1.4	4.9	109	2.0	9.4	41	2.1	3.1	16	2.1	2.2
2	204	4.3	6.6	101	4.9	8.5	42	5.1	3.9	17	5.1	2.7
3	203	4.0	7.5	105	4.3	8.3	40	4.4	2.4	18	4.4	1.8
4	199	4.5	3.7	103	4.7	7.8	39	4.9	3.7	23 8*	4.9 5.0	3.0 2.8
5	197	5.1	2.2	104	5.3	10.0	42	5.3	8.9	23 9*	5.3 5.4	6.2 5.8

\*  $\epsilon'$  peak.

### Effect of Orientation on Mechanical Relaxation Spectra

Orientation has a significant effect on the mechanical relaxation spectra of PET. In Figure 3, the loss modulus is shown as a function of temperature for three samples having similar crystallinities but markedly different levels of orientation. Data describing the relaxation maxima of five representative oriented samples are summarized in Table 4. Biaxial orientation substantially sharpens the relaxation maxima and produces a surprising splitting of the  $\beta$  and  $\delta$  peaks. Both of these variables may be extremely useful in explaining cryogenic ductility.)

As in the unoriented samples, structural characterization as well as more dynamic measurements at various orientations are underway in order to determine the mechanism of molecular motion at each relaxation maxima. This problem is both challenging and complex since six new relaxation maxima ( $\beta'$ ,  $\gamma$ ,  $\delta'$ ,  $\delta$ ,  $\epsilon$ ,  $\epsilon'$ ) have been uncovered during the past six months.

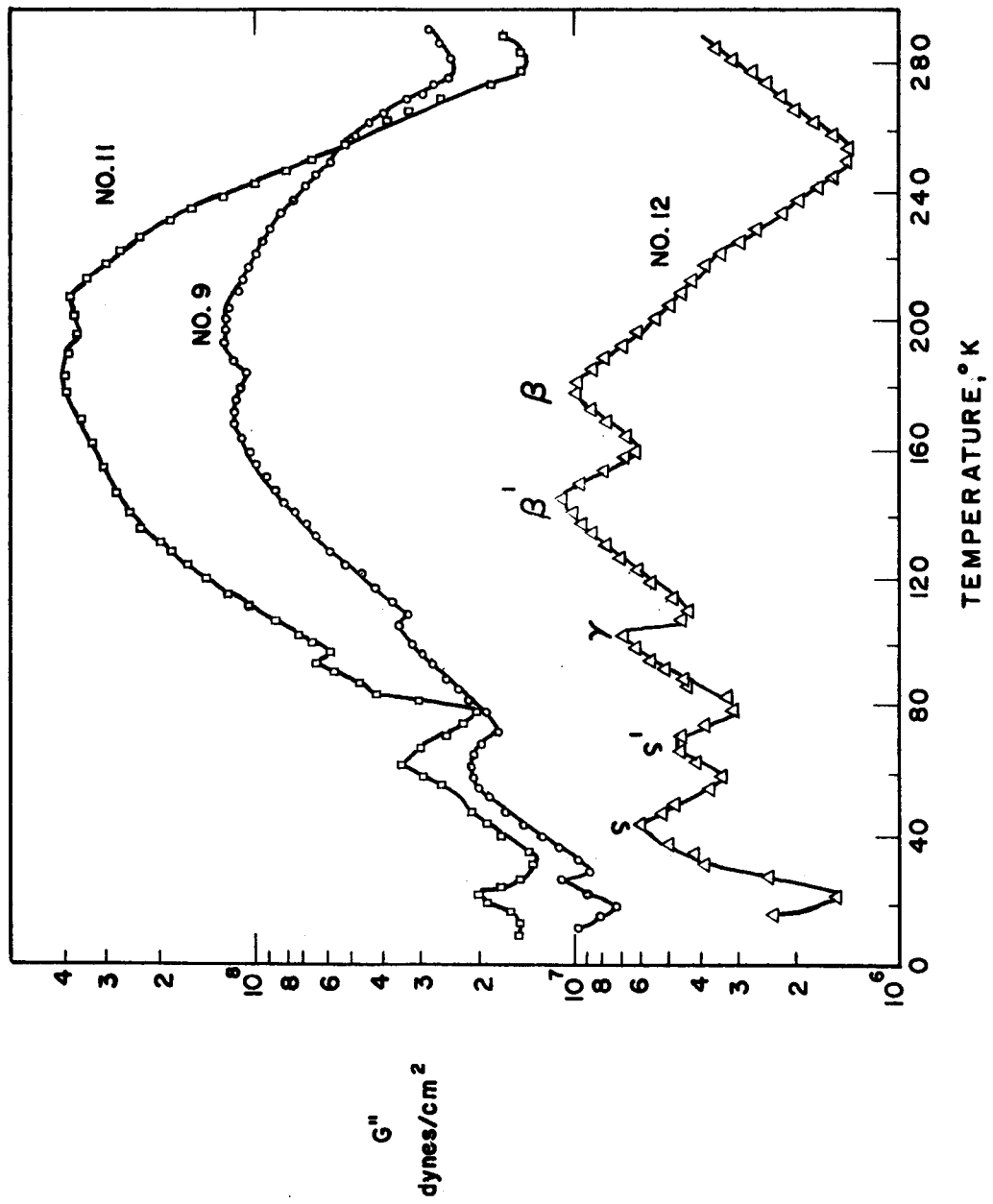


Figure 3.

Table 4  
Summary of Results Describing Relaxation  
Peaks Observed with Oriented PET Film

Sample No.	$\beta$ peak			$\gamma$ peak			$\delta$ peak			$\delta$ peak		
	T °K	G' $\times 10^{10}$	G'' $\times 10^8$	T °K	G' $\times 10^{10}$	G'' $\times 10^7$	T °K	G' $\times 10^{10}$	G'' $\times 10^7$	T °K	G' $\times 10^{10}$	G'' $\times 10^7$
8	198	5.4	2.8	96	5.6	6.2	64.0**	5.6	4.4	19.5	5.6	4.2
	171*	5.5	2.5				39.5	5.6	4.2			
9	200	2.9	1.3	105	3.1	3.7	60.0**	3.1	2.1	25.0	3.2	1.0
	172*	3.0	1.2									
10	189	82.0	7.6	97	8.2	4.3	62.0**	82.0	23.8	16.0	83.0	3.9
	159*	82.0	7.9				41.0	83.0	31.8			
11	204	8.7	3.9	94	9.6	6.8	63.0**	9.8	3.3	21.0	9.9	2.0
	179*	9.0	4.2				45.0?	9.8	2.0			
12	179	2.0	0.10	102	2.0	7.1	69.0**	2.0	4.6	?	?	?
	141*	2.0	0.086				43.0	2.0	6.2			

\*  $\beta'$  peak\*\*  $\delta'$  peak

## FIGURE CAPTIONS

- Figure 1. Logarithmic decrement as a function of temperature for two samples of amorphous PET.
- Figure 2. Shear modulus and loss modulus as a function of temperature at two different crystallinities. (Frequency c.p.s., solid line 53%, dashed line 17.2%).
- Figure 3. The effect of orientation on loss modulus as a function of temperature. ( $\square$  commercial Mylar, process history unknown, little orientation;  $\circ$  uniaxially oriented film;  $\bullet$  biaxially oriented PET film; Mylar C).
- Figure 4. Loss modulus as a function of temperature for various related glycol terephthalate polymers. ( $\bullet$  Polyethylene terephthalate, annealed at  $110^{\circ}\text{C}$ , 10 hrs.,  $\Delta$  Polyhexamethylene terephthalate, annealed at  $98^{\circ}\text{C}$ , 1 hr.,  $\square$  Polynonamethylene terephthalate, annealed at  $63^{\circ}\text{C}$ , 1 hr.)

## REFERENCES

1. Farrow, G., J. McIntosh and I.M. Ward, Makromol. Chem. 38, 147 (1960).
2. Bateman, J. R. E. Richards, G. Farrow, and I.M. Ward, Polymer, 1, 63, (1960).
3. Land, R., R. E. Richards, and I.M. Ward, Trans. Faraday Soc., 55, 225 (1959).
4. Illers, K. H., and H. Breuer, J. Colloid Sci., 18, 1 (1963).
5. Kawaguchi, T., J. Polymer Sci., 32, 417 (1958).
6. Kline, D.E., and J. A. Sauer, Polymer 2, 401, (1961).

N67-16089

Part II

MORPHOLOGY OF PET

by

G. Yeh and P. H. Geil

## ABSTRACT

A study has been made of the morphology of polyethylene terephthalate (PET), with primary emphasis on the morphology of the glass and the effect of strain-induced crystallization of the polymer. PET crystallizes from solution in the form of chain-folded fibrillar ribbons as in most solution-grown polymer crystals. The morphology of the glassy state is characterized by 75 Å ball-like structures in which the molecules are packed with some "order". Crystallization from glassy amorphous PET occurs by the formation of spherulites consisting of ribbon-like lamellae. The long period increases as measured by small angle x-ray scattering with annealing temperature but it decreases with time at a given annealing temperature. An interpretation is given for this decrease of long period with time. Strain-induced crystallization of PET occurs by alignment of the ball-like structures. Subsequent heat treatment of the strained material produces more complete alignment of the ball-like structures as well as perfection in the chain packing within the structures. A special technique, "Selected Area Small Angle Electron Diffraction", capable of resolving spacings up to 2000 Å has been developed in order to investigate the details of the morphology of oriented PET.

### Glassy, Amorphous State of PET

Both bulk and thin film samples were used in the present study. Bulk amorphous, glassy films were prepared by quenching a molten film in ice water. The surface was examined by replication electron microscopy. Thin films ( 500-1000Å) were prepared by a solution casting technique using a 1% trifluoroacetic acid (TFA) solution. Only fresh solutions were used. The films are transparent and are amorphous according to their electron diffraction patterns (Figure 4). These films are thin enough to permit direct transmission studies in the electron microscope.

Examinations of solution-cast amorphous thin films showed that they contained ball-like structures between 45 Å and 100 Å in size. Figure 5 gives an example of ball-like structures present in amorphous bulk material. The ball size occurs at about 78 Å for the solution cast materials and about 75 Å for the amorphous bulk material. On the average the solution-cast thin films always have slightly larger diameter balls than the bulk samples but this is the only visible difference between the two preparations. Therefore the majority of the work was conducted on thin films which allowed direct transmission studies on both shadowed and unshadowed specimens, and consequently meaningful results could be obtained. It should be mentioned that there was no observable changes in ball size using two different solution-casting systems, m-cresol and TFA.

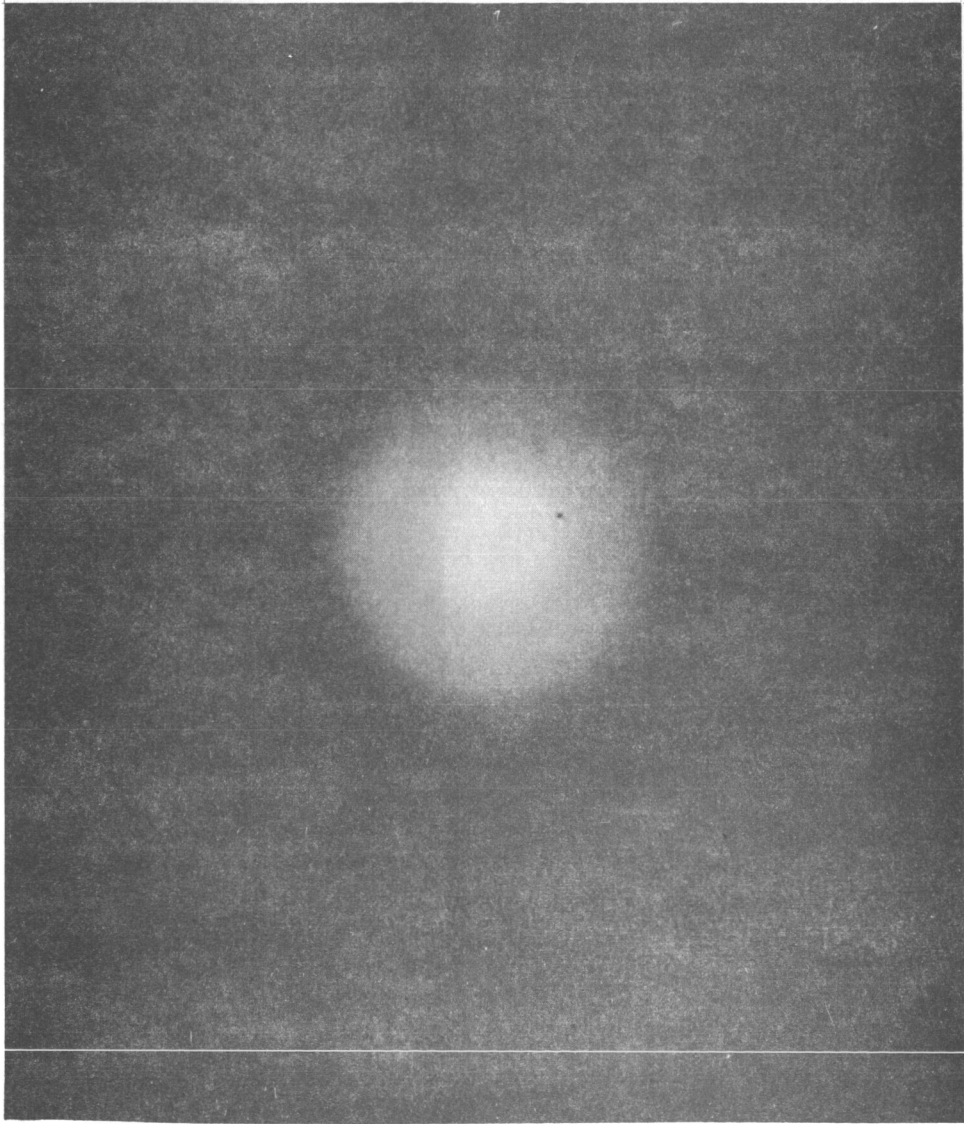


Figure 4.

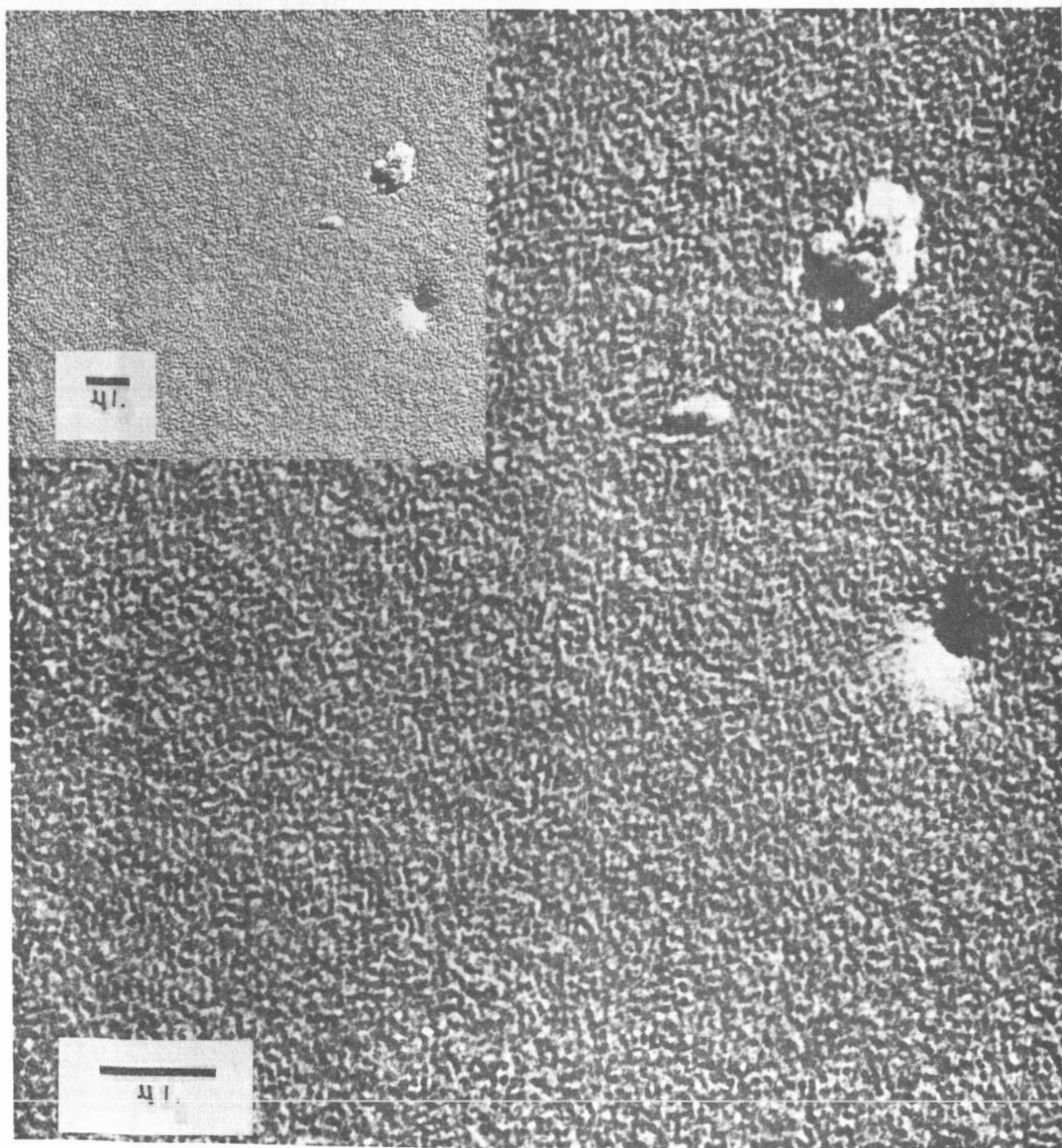


Figure 5.

However, no attempts were made to see if the ball size changes with the quenching conditions employed in the bulk systems.

The ball-like structures are observable as regions of fair contrast under bright field illumination in the thin film samples (Figure 6, top), indicating a fluctuation in mass density in the sample in this size range. The dark field micrograph of the corresponding area obtained by using a portion of the innermost diffuse scattering ring ( $d$  spacing =  $3.7 \text{ \AA}$ ) is shown in Figure 6, bottom. Small bright regions of the size of the ball-like structures or smaller are seen all over the field. These are the scattering ring, indicating that the ball-like structures have some degree of order within them.

#### Effect of Annealing Glassy, Amorphous PET Near or Below $T_g$ .

All samples were prepared by annealing in a test tube placed in a temperature-controlled oil bath. On annealing at temperatures below  $T_g$ , the ball-like structures tend to move, aggregate, and align. Depending on the annealing temperature and time and the film thickness, large structures suggesting the initial growth stages of spherulites may be formed.

Figure 7 is a surface replica of bulk amorphous material which had been annealed for 6 days at  $60^\circ\text{C}$  (i.e.,  $5^\circ\text{C}$  below  $T_g$ ). The  $100 \text{ \AA}$  size

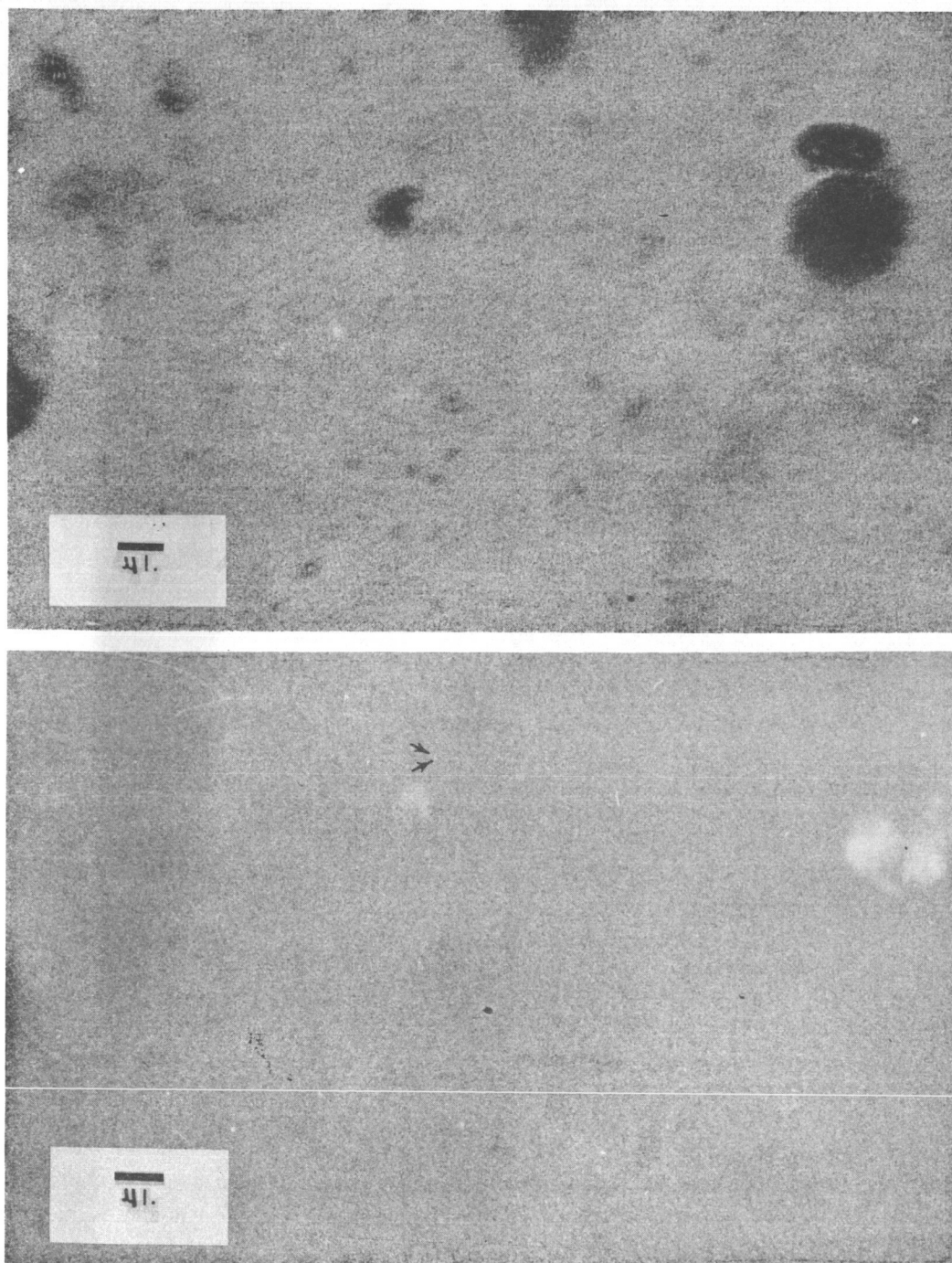


Figure 6.

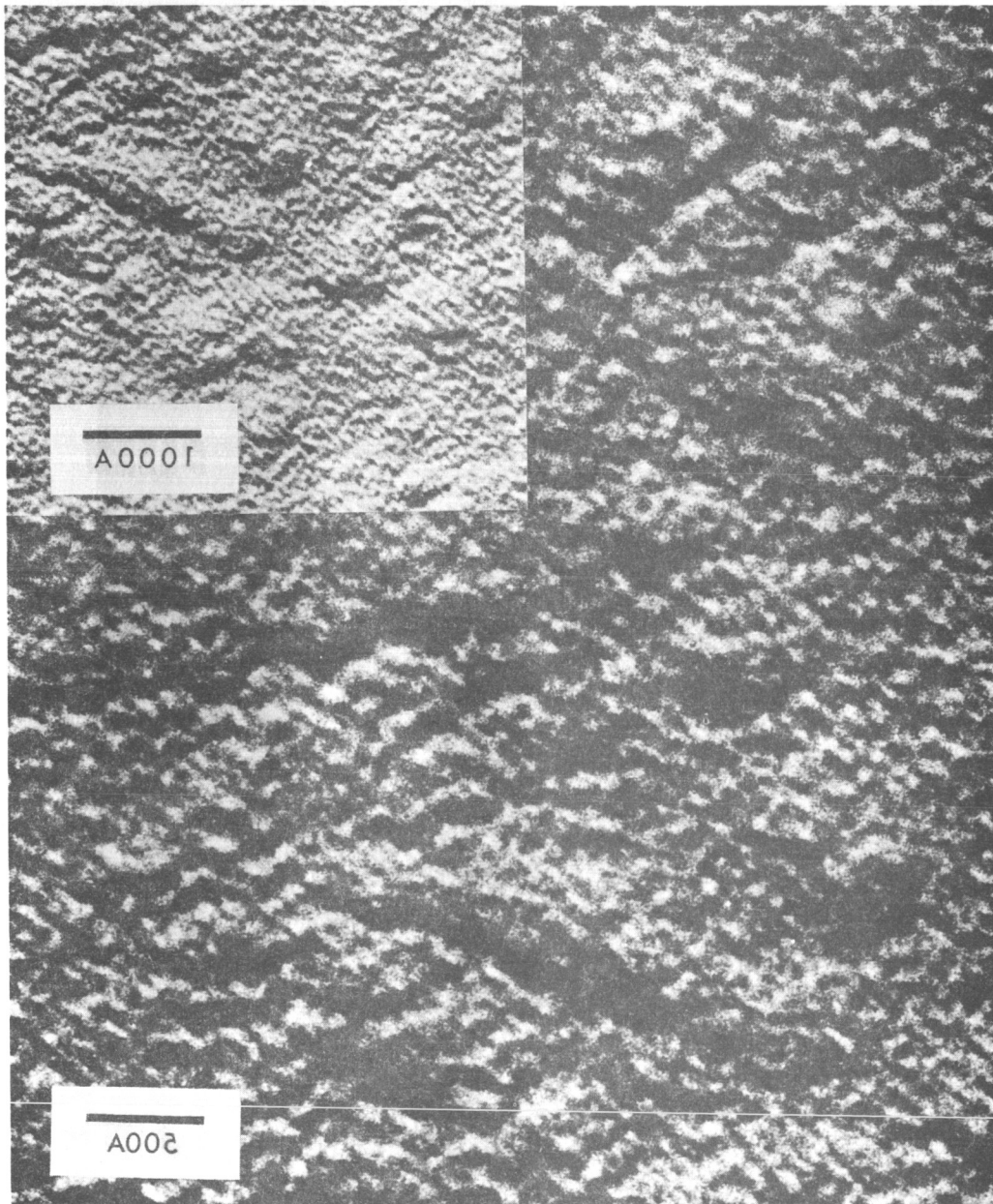


Figure 7.

structures are seen aggregated in many places forming larger more or less spherical patches about 5-10 balls in diameter. The size of the individual ball remains about the same.

The results from thin film work are more striking and, in addition, more informative since diffraction studies can be made. The type of structures observed at an annealing temperature of  $56^{\circ}\text{C}$  for 4 days are shown in Figure 8. Aggregates of ball-like structures seem to form branches off a tree. The ball-like structures do not have any particular orientation along any one branch. At an annealing temperature of  $60^{\circ}\text{C}$  small structures resembling the initial growth stages of spherulites were observed all over the surface and at the same time, too, the  $(111)$  and  $(011)$  reflections started to appear (Figure 9). These spherulites do not increase very much in size ( $\sim .5$  micron) even after 7 days of annealing at this temperature. However, their size increases drastically at  $66^{\circ}\text{C}$  or near the  $T_g$  of PET (Figure 10). Furthermore, the ball-like structures become quite oriented with respect to each other in some places within the spherulitic fibrils. They tend to align in rows normal to the fibril axis.

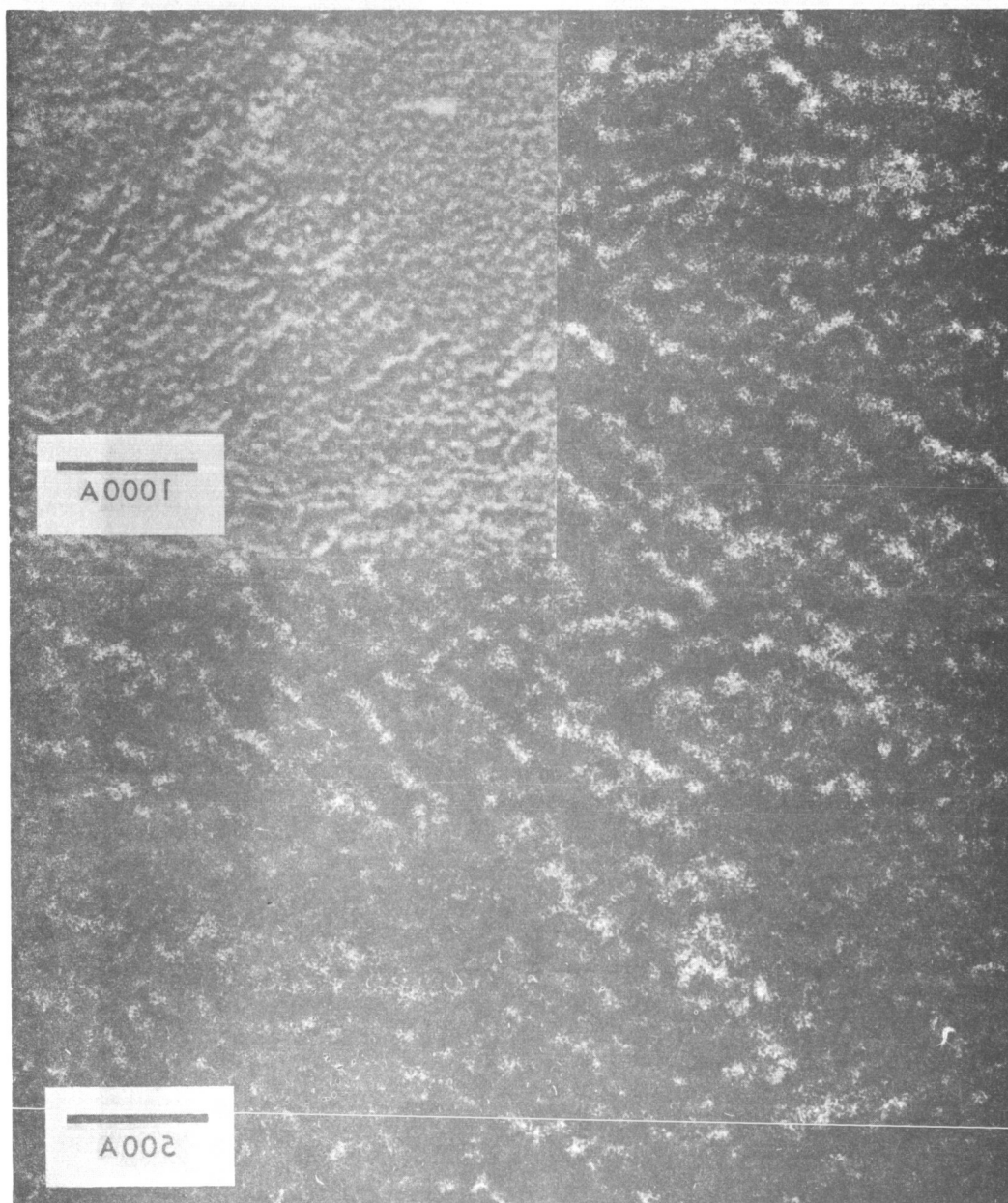


Figure 8.

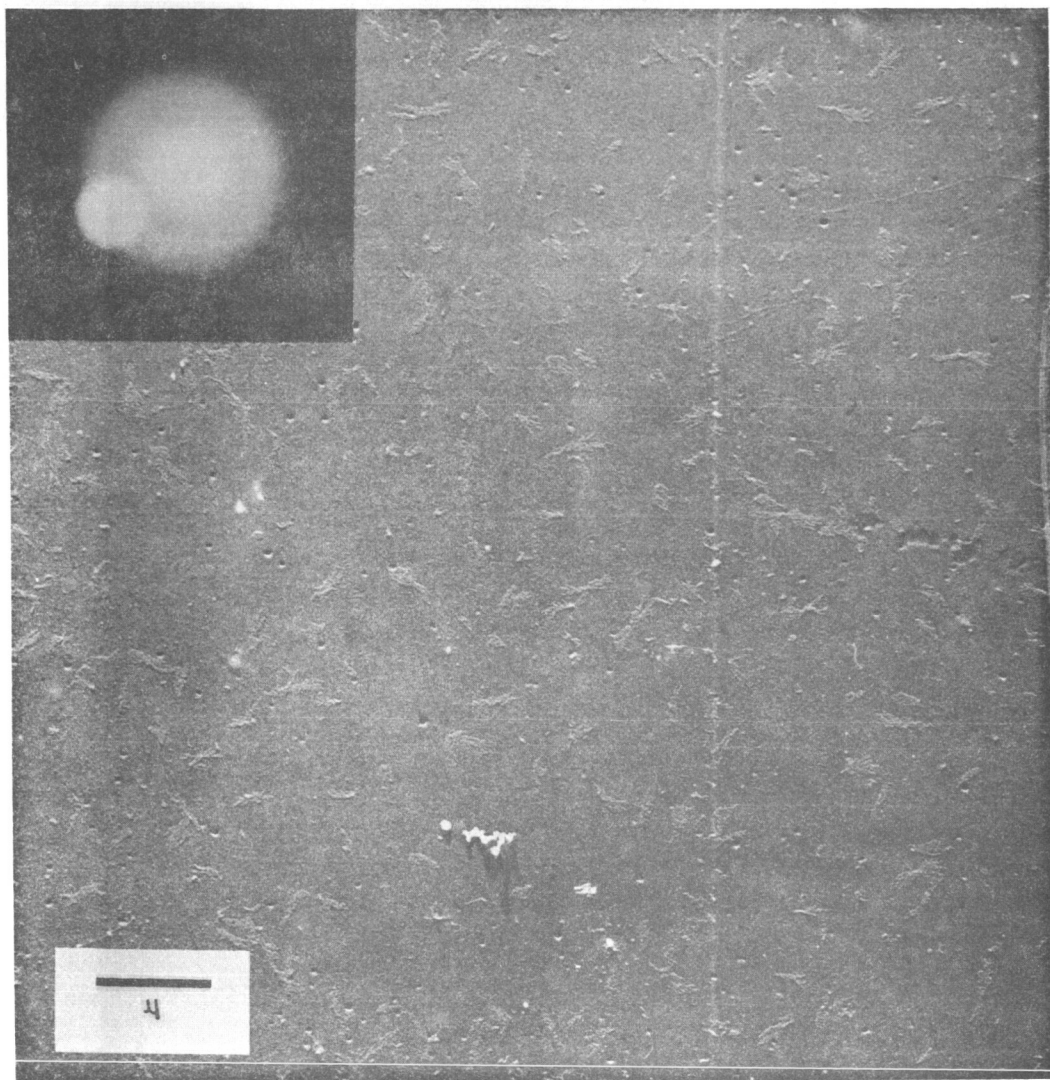


Figure 9.

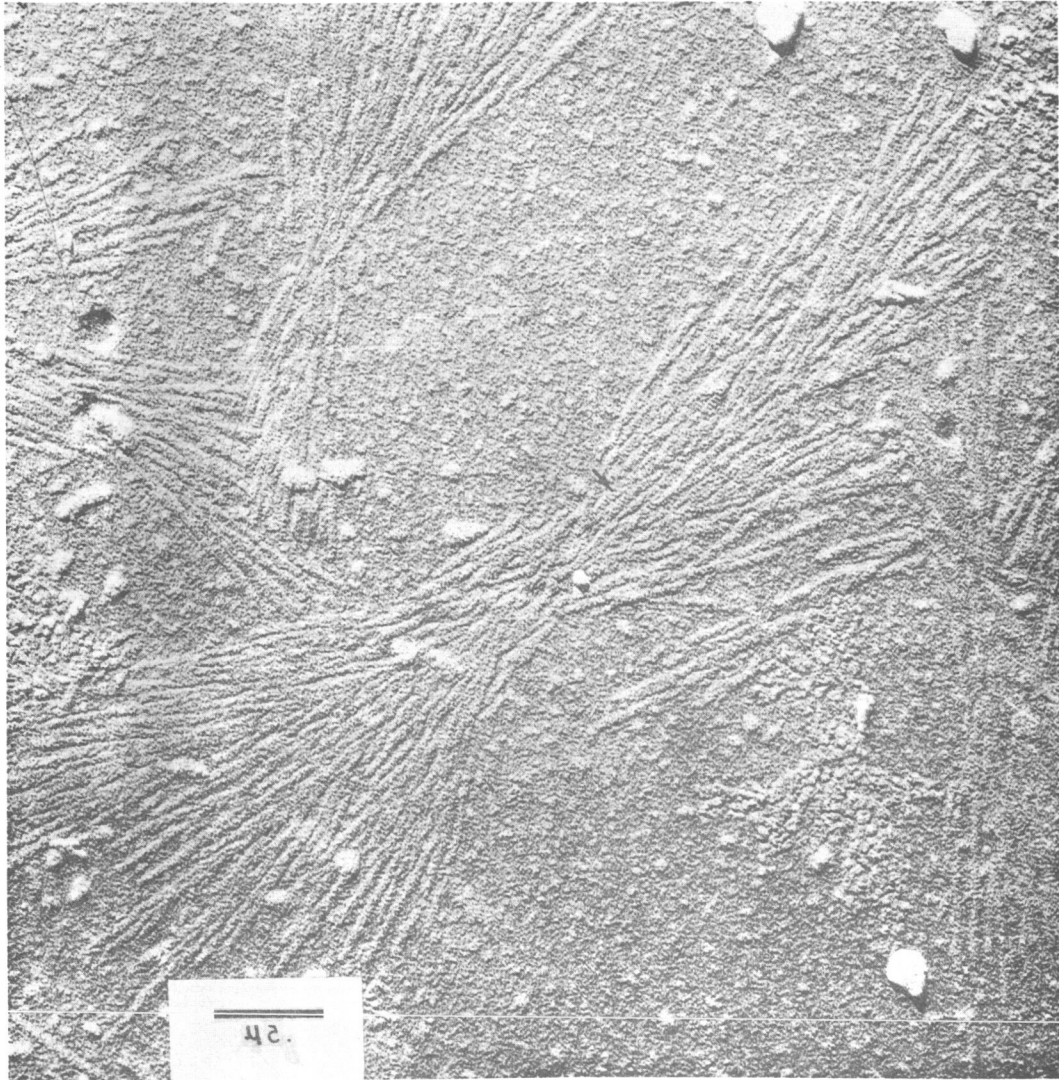


Figure 10.

### Conclusion

The observation of movement of the ball-like structures at temperatures well below  $T_g$  ( $10^{\circ}\text{C}$  below) is a significant finding of this portion of research on polyethylene terephthalate. The significant flexibility of the polymer even at temperatures well below  $T_g$  is therefore suggested as resulting from some energy absorbing mechanism provided by the "ordering" and "disordering" of the molecules within the balls and/or the relative motion between the balls. Further confirmation of this suggestion is going to require the finding of some means of varying the size of and the strength of cohesion between the balls in a known preparation.

## FIGURE CAPTIONS

- Figure 4. Electron diffraction pattern of solution-cast thin film showing the typical amorphous liquid-like PET diffraction pattern.
- Figure 5. Replica surface of amorphous bulk PET showing the presence of ball-like structures.
- Figure 6. Top: Bright field electron micrograph of an amorphous thin film showing regions of fair contrast due to presence of ball-like structures. Bottom: Corresponding dark field electron micrograph obtained by using a portion of the innermost diffuse ring. Note the slightly higher magnification of the dark field micrograph.
- Figure 7. Replica surface of amorphous bulk PET after annealing at 60°C for 6 days. Spherical patches consisted of 5-10 balls in diameter are seen.
- Figure 8. Surface structure of amorphous thin film after annealing at 56°C for 4 days. Aggregations of ball-like structures linked together are seen in some areas.
- Figure 9. Surface structure of amorphous thin film after annealing at 60°C for 1 day. The whole surface is covered with incipient spherulitic structures. A diffraction pattern obtained from a similar area shows the presence of  $(\bar{1}11)$  and  $(011)$  reflections. A portion of the diffraction pattern was double-exposed using the objective aperture for dark field studies.
- Figure 10. Spherulites formed by annealing an amorphous thin film at 66°C for 6 days. The ball-like structures within the fibrils tend to align in rows normal to the fibril axis (see arrow).

N67-16090

Part III

INFRARED STUDIES OF

SOLVENT INDUCED CRYSTALLIZATION

by

J. L. Koenig and B. Hickle

## Experimental

The effects of solvent and dip time on the crystallinity of PET and Mylar samples were studied. Acetone and Toluene were chosen as the solvents to be used because of results obtained by Moore and Sheldon<sup>(1)</sup> on the rate of induced crystallization, and also because of their low boiling points for easier drying.

Samples were prepared by cutting the films into 1 1/2 inch squares and placing them in an 80°C vacuum oven overnight to dry. The samples were then removed from the oven and dipped at room temperature. They were then marked and placed in an 80°C vacuum oven overnight.

The samples were removed from the oven and cut in half, half being heat set in a 140°C vacuum oven for half an hour. All samples were run on the Perkin-Elmer 521 Infra-Red Spectrophotometer and absorbance values were calculated from baselines employed in Hannon's work with PET.

The effect of dip time on the 973  $\text{cm}^{-1}$  band (crystalline) and the 988  $\text{cm}^{-1}$  band (fold) for both heat set and non-heat set samples are shown in the following graphs. All values are divided by the 795  $\text{cm}^{-1}$  band (internal thickness) to make the various samples comparable. The error in the absorbance values was calculated to be 0.1 absorbance units.

## Discussion

An examination of Figures 11, 12, 13, and 14 indicates that several conclusions can be drawn about solvent-induced crystallization of PET.

The amount of solvent-induced crystallinity depends on the dip-time or equivalently on the amount of solvent in the amorphous film. The time-dependent increase in crystallinity in presence of solvent hit below the glass transition is similar to the time-dependent behavior of heat-induced crystallinity at temperatures above the glass transition in the absence of solvent. Heat setting of samples which had been dipped produced an additional increase in crystallinity as expected but the initial decrease for very short dip times is anomalous.

Acetone-dipped films had a higher crystallinity for equivalent dip-times than toluene-dipped films. Since acetone is a better solvent than toluene, this is not an unexpected result.

The amount of solvent-induced crystallinity in commercial mylar samples is considerably lower due to the high initial crystallinity. Due to the small changes in crystallinity very little difference was observed between the two solvents. Heat setting of the dipped commercial films did not produce any major differences.

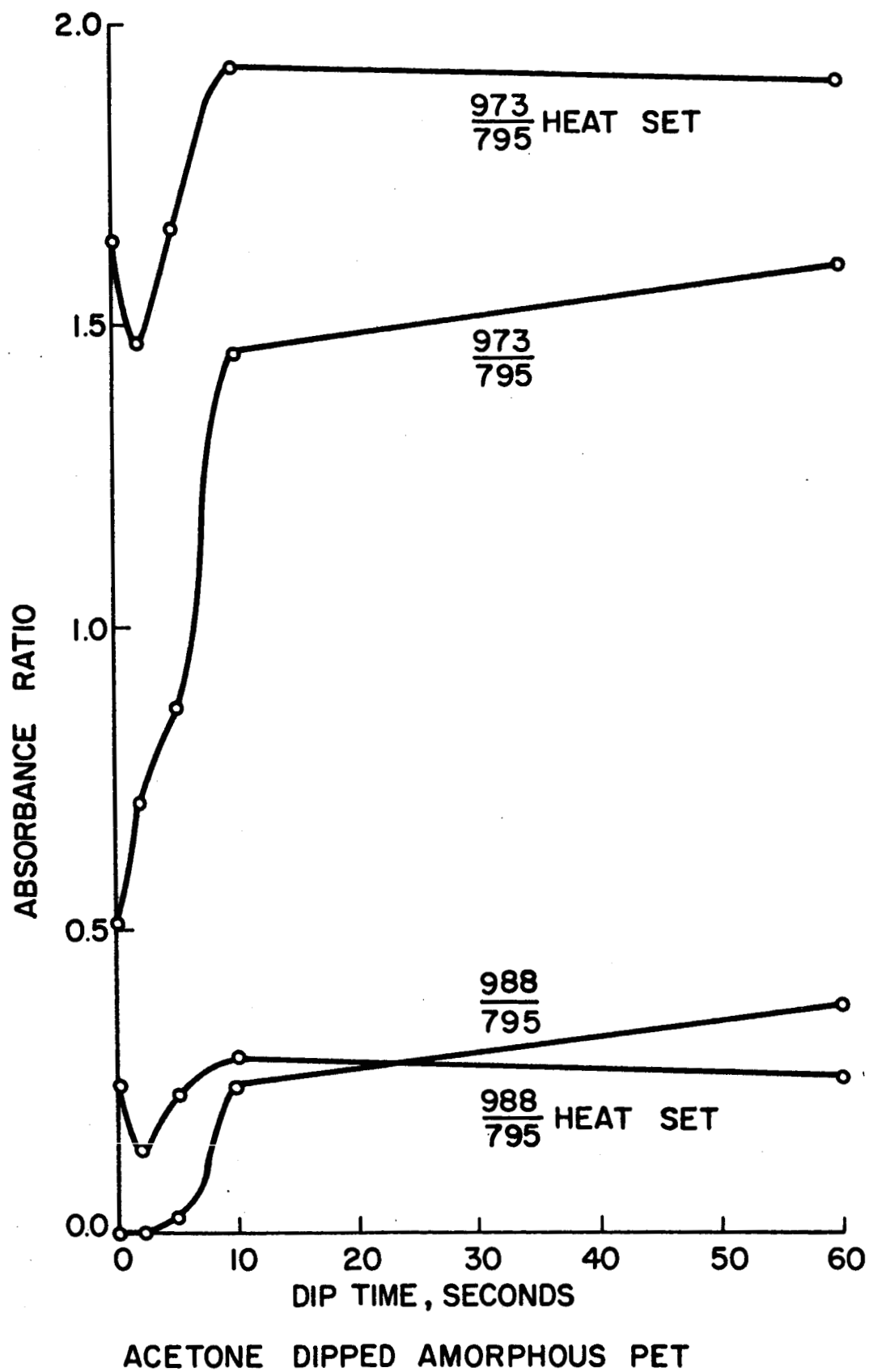


Figure 11.

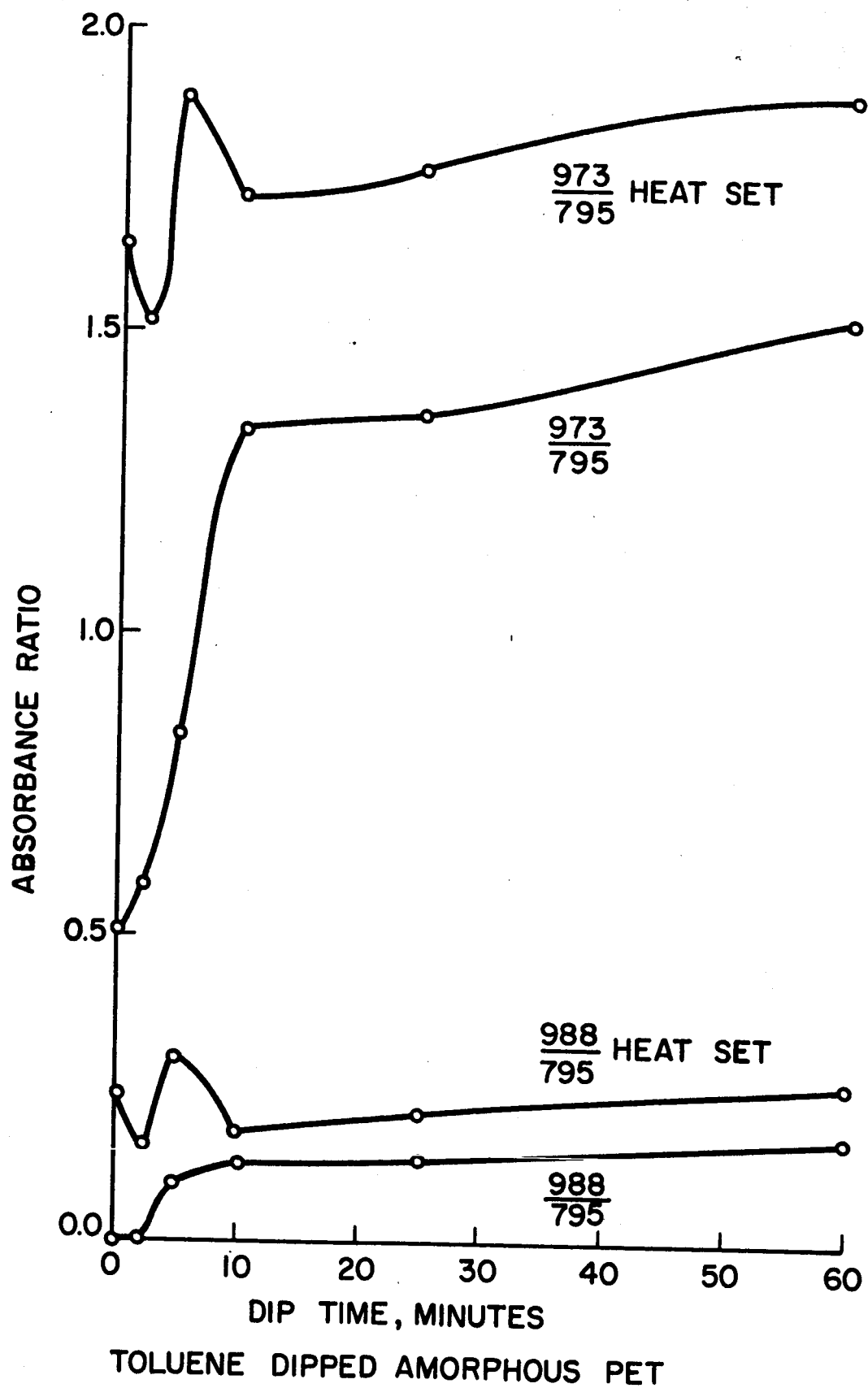
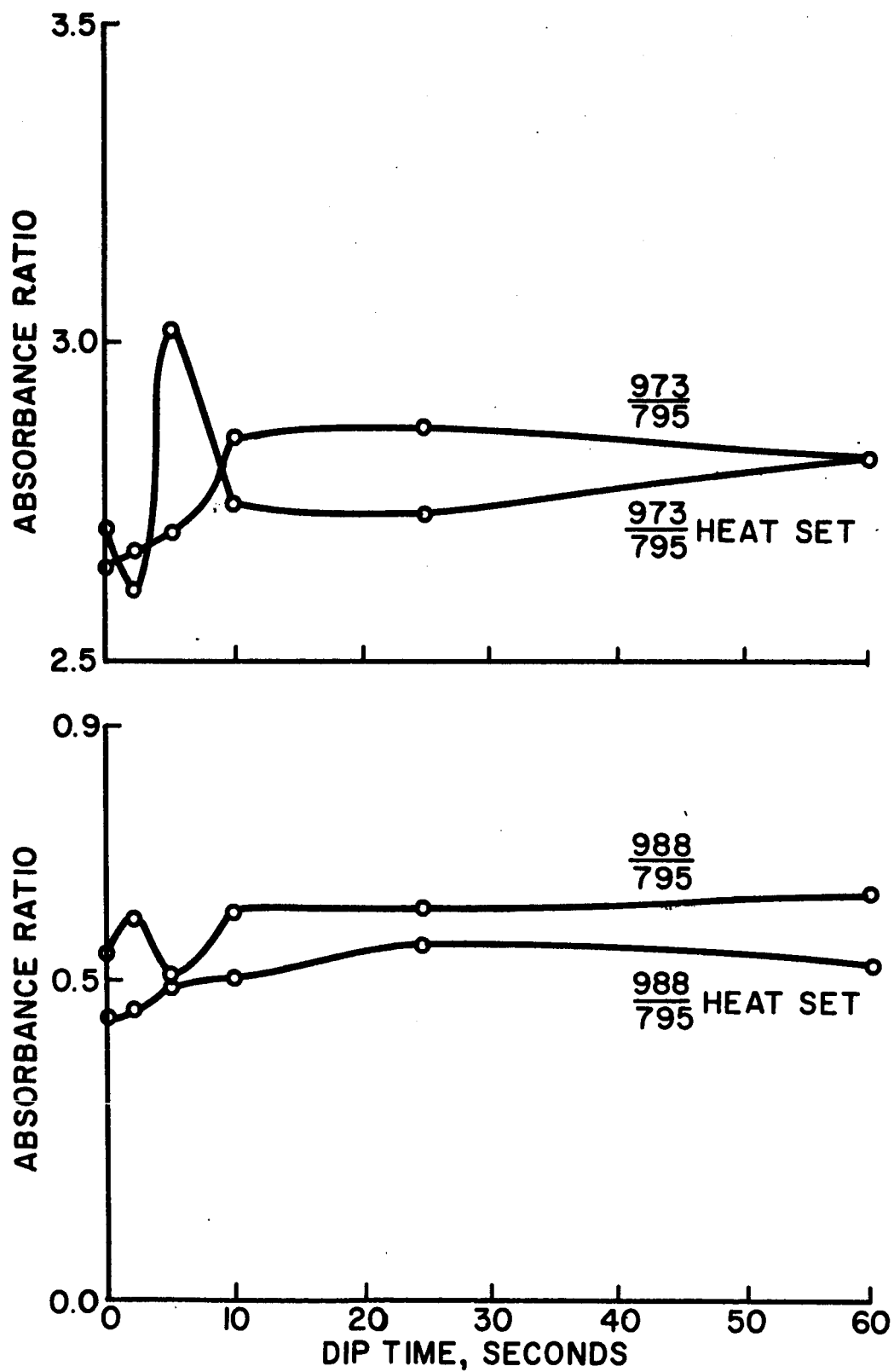


Figure 12.



ACETONE DIPPED COMMERCIAL MYLAR

Figure 13.

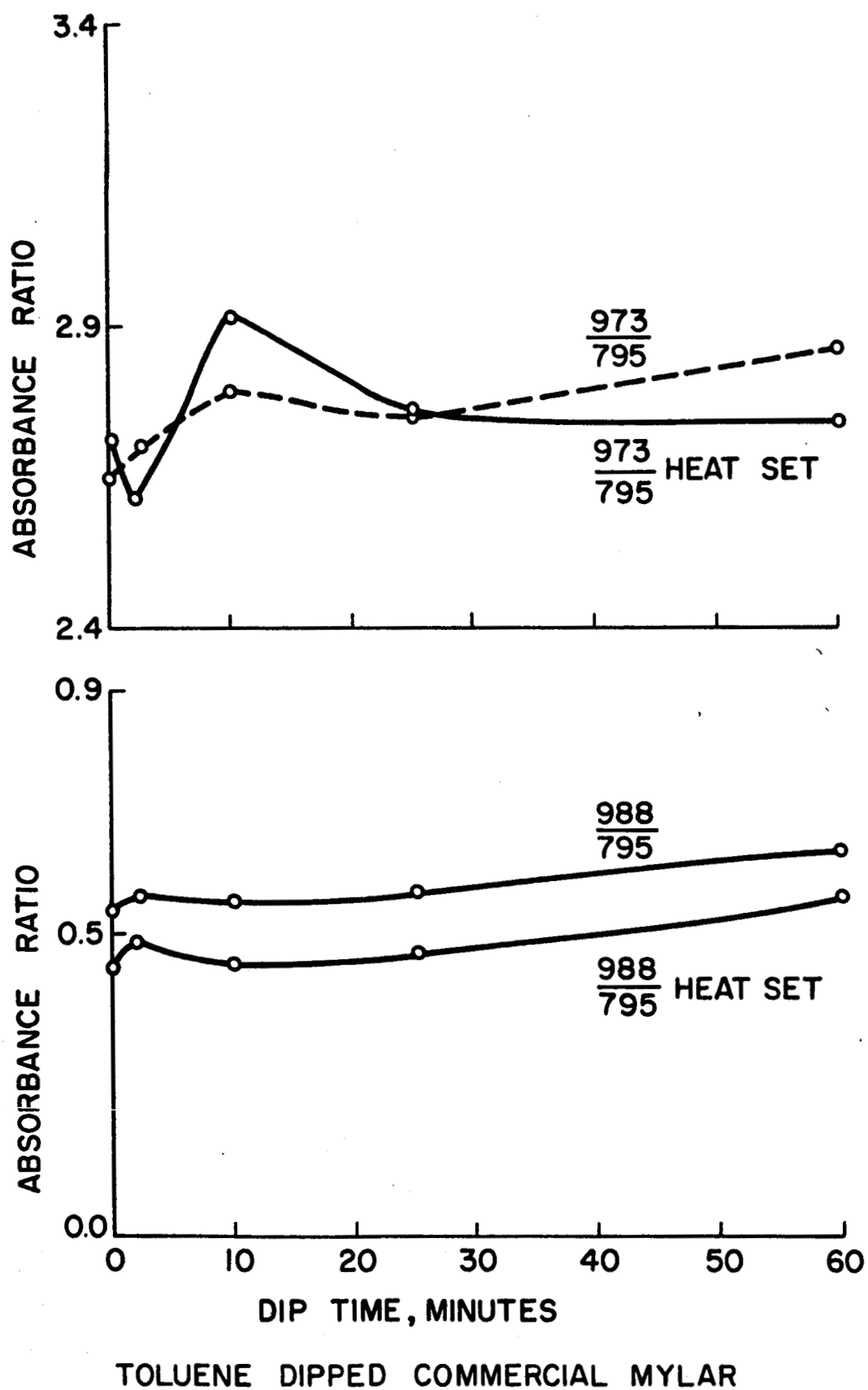


Figure 14.